

Optical Damage, Nonlinear Transmission, and Doubling Efficiency in LiIO_3

E. W. Van Stryland, William E. Williams,
M. J. Soileau, and A. L. Smirl

Center for Applied Quantum Electronics
North Texas State University
Denton, Texas 76203

Laser-induced damage thresholds of single crystal LiIO_3 have been studied using picosecond pulses at $1.06 \mu\text{m}$ and $0.53 \mu\text{m}$. These thresholds depend on wavelength, crystal orientation, and on the number of times the sample has been irradiated. In addition, the doubling efficiency at high irradiance levels was observed to be a decreasing function of irradiance beyond a critical value. We present evidence to show that this results from the onset of optical parametric down conversion. In separate nonlinear transmission studies, reversible nonlinear transmission of $1.06 \mu\text{m}$ light was measured, and in self-diffraction experiments, both reversible and irreversible optically-induced complex index of refraction changes at $0.53 \mu\text{m}$ were observed.

Key words: LiIO_3 , laser induced damage, second harmonic generation, transient gratings, nonlinear absorption.

1. Introduction

Is it well known that the large nonlinear coefficient of lithium iodate (LiIO_3) makes it an attractive candidate for applications where second harmonic generation is required [1]. Consequently, we have begun a study of the laser-induced damage (LID) thresholds of this material and of the mechanisms that limit its second harmonic conversion efficiency. Here, we report the results of five separate but related experiments in this area. (1) In the first of these (Sec. 2), we measure the laser-induced damage thresholds of single crystal LiIO_3 using picosecond pulses at $1.06 \mu\text{m}$ and $0.53 \mu\text{m}$. We find that the LID thresholds vary with wavelength, pulsewidth, crystal orientation, and the number of times that the sample is irradiated. Specifically, we observe that the sample is more easily damaged when green ($0.53 \mu\text{m}$) light is present and that the damage is initiated by some nonlinear absorption process, which is more efficient at $0.53 \mu\text{m}$. The sample also damages more easily with repeated irradiations at both wavelengths. We thus obtain a single shot and a multishot threshold. (2) Next (Sec. 3), we determine the dependence of the second-harmonic conversion efficiency of $1.06 \mu\text{m}$ radiation to $0.53 \mu\text{m}$ radiation on incident irradiance. We find that the efficiency initially increases with excitation level to a maximum at approximately 50% and then decreases. This decrease is consistent with one of three mechanisms: (a) any absorption processes of the second harmonic or nonlinear absorption of the fundamental, (b) a nonlinear refractive index change that destroys the exact phase-matching conditions, or (c) the onset of parametric down conversion. In an effort to identify the mechanism limiting the conversion efficiency and to identify the nonlinear mechanism responsible for the onset of damage, we perform three related studies. (3) We first measure (Sec. 4)

the nonlinear transmission of LiIO_3 at both $0.53 \mu\text{m}$ and $1.06 \mu\text{m}$ (under non-phase-matched conditions). We observe multiphoton absorption of the $1.06 \mu\text{m}$ radiation (the order appears to be greater than four) at irradiances well above the multishot threshold for damage. No nonlinear absorption at $0.53 \mu\text{m}$ is resolved up to the multishot damage threshold for green light. The onset of the observed nonlinear absorption of the fundamental occurs at too high an irradiance to account for the observed decrease in the conversion efficiency. (4) Although no nonlinear absorption or index changes are observed at $0.53 \mu\text{m}$ in the transmission studies just described, both reversible and irreversible changes in the complex refractive index are observed at $0.53 \mu\text{m}$ by using a more sensitive background-free two-pulse self-diffraction technique (Sec. 5). (5) Finally (Sec. 6), we measure the dependence of the spatial beam profile of the second harmonic on the fundamental irradiance. From the distortion in the $0.53 \mu\text{m}$ beam profile for large irradiances we conclude that down conversion is responsible for the decrease in conversion efficiency with increasing irradiance.

2. Damage Thresholds

The initial experimental arrangement to be used in damage and conversion efficiency experiments is shown in figure 1. The laser source was a passively mode-locked $1.06 \mu\text{m}$ Nd:YAG laser that produced Gaussian spatial mode pulses of temporal width externally variable between 40 and 200 psec (FWHM). Details of the experimental apparatus are given in Ref. [2] included in these proceedings. The laser beam traversed the LiIO_3 with a uniform beam radius of $440 \mu\text{m}$ (all spot sizes are quoted as the half width at the e^{-2} point in irradiance). When $0.53 \mu\text{m}$ light was required, a second doubling crystal (KD*P) was inserted prior to the sample. The collimated $0.53 \mu\text{m}$ beam had a spatial width of $310 \mu\text{m}$ in the LiIO_3 . In this case, residual $1.06 \mu\text{m}$ light was removed with polarizers and $1.06 \mu\text{m}$ blocking filters.

The laser-induced damage thresholds (LIDT) for LiIO_3 were measured at $1.06 \mu\text{m}$ and $0.53 \mu\text{m}$ for various crystal orientations and pulsewidths. Both the single shot or 1 on 1 thresholds (i.e., each site irradiated only once) and multiple shot or N on 1 thresholds (i.e., each site irradiated many times with irradiance levels well below the single-shot damage threshold) were measured. The onset of damage was determined by observing both increased scattering of coaxial HeNe light and by observing other visible sample changes with a long working distance microscope. In LiIO_3 , both damage signatures occurred simultaneously. The LIDT is defined as that fluence or irradiance which produces visible damage with 50% probability as determined by the method of Porteus *et al.* [3]. The experimental uncertainties in the LIDT measurements are indicated by the dotted lines in Tables I and II, and they include the relative uncertainty as determined in ref. 3, absolute energy calibration error and the uncertainty in the spot size measurements.

The results of the damage measurements using $1.06 \mu\text{m}$ light are presented in Table I. The LIDT was measured for 45 psec and 120 psec (FWHM) pulses with a spot size of 0.44 mm . Both the fluence and the corresponding irradiance threshold are shown. The single shot (1 on 1) LIDT fluence for front surface damage to the sample was approximately 1.3 J/cm^2 for both pulsewidths. For a beam radius that is constant throughout the sample, one would expect normally to see rear surface damage at lower fluence levels than front surface damage since the field at the exit surface should be approximately 30% greater than at the front surface for transparent samples. However, in this case (as we shall discuss in Sec. 4), depletion of the beam by nonlinear processes reduced the fluence at the rear surface by as much as a factor of 8 for input irradiance near the LIDT levels. As expected, the surface damage thresholds were independent of crystal orientation (i.e., whether or not the crystal was phasematched).

Because single shot damage first occurred on the sample front surface, the single shot bulk damage threshold could not be determined. However, approximately 20% of the shots at a fluence of 1.3 J/cm^2 resulted in bulk damage just below the front surface. From these measurements, we estimate a lower limit for the bulk, single shot, damage threshold to be 1.3 J/cm^2 .

Table I also contains the results of the multiple shot or N on 1 measurements for $1.06 \text{ }\mu\text{m}$ light for both phase-matched and non-phase-matched conditions. For the non-phase-matched (NPM in Table I) configuration, the LiIO_3 crystal was rotated about the laser beam propagation axis to an orientation 90° from the phase-matched orientation. In this configuration, no $0.53 \text{ }\mu\text{m}$ light was visible. Each site was irradiated at levels far below the single shot threshold and slowly increased until damage was observed. Multiple shot damage was always initiated in the bulk, and the thresholds were determined to be substantially below the lower limit of 1.3 J/cm^2 found for the 1 on 1 experiments. Maximum lowering of the LIDT was achieved after approximately 50 irradiations at 0.2 J/cm^2 . Notice that the N on 1 thresholds are considerably lower for the crystal oriented to produce second harmonic light. The $1.06 \text{ }\mu\text{m}$ to $0.53 \text{ }\mu\text{m}$ conversion efficiency (see Sec. 3) was of the order of 50% for the input irradiance that produced breakdown. These results suggest that the green light may be responsible for damage under phase-matched conditions. To confirm this suggestion, we measured the multiple-shot LIDT for $0.53 \text{ }\mu\text{m}$ radiation. For these measurements, a KD*P second-harmonic crystal was inserted following the Nd:YAG laser, and all residual $1.06 \text{ }\mu\text{m}$ light was removed, as described above. Indeed, the results (presented in Table II) indicate that when $0.53 \text{ }\mu\text{m}$ radiation is present, it is primarily responsible for initiating damage. Because of the role of the green light in determining the LIDT when the crystal is phase matched, we investigate the dependence of the second harmonic conversion efficiency on irradiance in the next section.

In addition, the lowered threshold for multishot irradiation is indicative of the formation of microscopic defects that eventually absorb enough energy to cause crystal fracture (what we observe as LID). This may be similar to the irreversible absorption changes seen in NaCl at $1.06 \text{ }\mu\text{m}$ (Wu *et al.* these proceedings) [4] or to a charge migration or photorefractive effect reported in other materials such as BaTiO_3 [5]. We conclude that these defects must be produced by a non linear process since no amount of irradiation at very low intensities causes a lowering of the damage threshold. Also the defects appear to be more efficiently produced by $0.53 \text{ }\mu\text{m}$ light as shown by the much lower multishot threshold at this wavelength. To investigate this supposition, we have also monitored the transmission of both $1.06 \text{ }\mu\text{m}$ light and $0.53 \text{ }\mu\text{m}$ light (no $1.06 \text{ }\mu\text{m}$ light present) as a function of the incident irradiance (Sec. 4). Similar multiple shot damage threshold changes have been observed previously at $0.69 \text{ }\mu\text{m}$ [6].

3. Doubling Efficiency in LiIO_3

In the determination of the damage thresholds at $1.06 \text{ }\mu\text{m}$ with the crystal in the angle phase matched orientation, we also monitored both the transmission at $1.06 \text{ }\mu\text{m}$ and the harmonic conversion efficiency (i.e. energy at $0.53 \text{ }\mu\text{m}$ divided by incident $1.06 \text{ }\mu\text{m}$ energy). Figure 2 shows both the transmission and conversion efficiency as a function of input $1.06 \text{ }\mu\text{m}$ irradiance for 40 psec (FWHM) pulses. Each data point is the average of 5 laser firings. The five data points at the highest irradiance were taken after GW was observed. The efficiency increases rapidly at low irradiance, reaches a maximum at $\sim 3 \text{ GW/cm}^2$, corresponding to an efficiency of 50%, and then decreases for higher incident irradiance levels (although the second harmonic energy continues to increase slowly). An identical experiment was performed using $\sim 140 \text{ psec}$ (FWHM) pulses that reproduced the data of figure 2

up to 3 GW/cm^2 where the sample damaged. Physical mechanisms that produce a theoretical fit to such a turnover in efficiency include nonlinear absorption of the second harmonic, [7,8] nonlinear refractive index changes that result in loss of phase matching at high irradiance levels, [7,8] and parametric down conversion of the $0.53 \mu\text{m}$ light [9,10]. To distinguish the contributions of these separate mechanisms, we performed three related measurements, to be described below.

4. Nonlinear Transmission Measurements

The transmission of the LiIO_3 at $1.06 \mu\text{m}$ was measured with the sample oriented such that no second harmonic was produced. This data for 45 psec pulses is shown in figure 3 as a plot of the inverse third power of the transmission versus the cube of the incident irradiance. The data is plotted in this manner to investigate whether four photon absorption might explain the results. Neglecting the Gaussian transverse structure of the beam, four photon absorption should yield a straight line on such a graph [2]. Integrals over the Gaussian spatial and temporal profiles tend to make the line curve downward as explained in ref. 2 of these proceedings. The curvature is upward indicating that the nonlinearity is of an order higher than four. We cannot account for the order of the nonlinearity even when the absorption caused by the subsequent photogenerated carriers is included. It is important that we emphasize that the data points are single laser firings and only a few shots were taken because the sample damaged more easily after each shot. The highest irradiance data point was taken first and the irradiance decreased with each subsequent shot. A final data point was taken at an increased irradiance to observe any possible hysteresis; none was observed for this small number of laser firings. Note also that several sites had to be irradiated to obtain the data shown, since many sites damaged on the first shot. All the data shown were obtained at irradiance levels near to or above the multishot damage threshold. (The single shot surface threshold is 27 GW/cm^2). This transmission data was taken with a $1.06 \mu\text{m}$ spike filter in front of the detectors. The possibility of conversion of the $1.06 \mu\text{m}$ light to other frequencies is not excluded although no visible light was observed.

The transmission of the LiIO_3 was also measured at $0.53 \mu\text{m}$ for both a phase-matched and non-phase-matched geometry. When great care was taken to eliminate all of the residual $1.06 \mu\text{m}$ light, no nonlinear transmission of the $0.53 \mu\text{m}$ light was observed up to the multishot damage threshold. These measurements determine an upper limit for the two-photon absorption coefficient at $0.53 \mu\text{m}$ of 0.03 cm/GW [11]. We were unable to obtain transmission at irradiances significantly above the multishot threshold as was done with $1.06 \mu\text{m}$ light, since our source of $0.53 \mu\text{m}$ radiation was not sufficiently intense. Whenever the crystal was in the phase-matched orientation and any residual $1.06 \mu\text{m}$ was allowed to strike the sample along with the $0.53 \mu\text{m}$ light, it was amplified depleting the $0.53 \mu\text{m}$ beam - a clear indication of parametric down conversion [9].

We also studied the spatial profile of the transmitted beams in the far field at both $0.53 \mu\text{m}$ and $1.06 \mu\text{m}$ as a function of incident irradiance at the same wavelength. These measurements were performed in the non-phase matched configuration. In this geometry, we could easily distinguish a half-wave distortion in the beam profile caused by self-focusing or defocusing. For a 0.5 cm -thick sample, this means that we should be able to detect a change in index on the order of 10^{-4} . No detectable distortion was observed up to the multishot damage thresholds.

From these two types of nonlinear transmission measurements, we conclude that any induced change in either the absorption coefficient or index of refraction is far too small to account for the turn over in the diffraction efficiency as displayed in figure 2.

5. Irradiance Dependent Complex Refractive Index Changes

The sensitivity of the nonlinear transmission measurements discussed in the previous section was limited by the large background signal present. That is, we were attempting to measure a very small change in a large signal. In this section, we describe the use of a more sensitive background-free self-diffraction technique to measure both transient and permanent optically-induced changes in the complex index of refraction at $0.53 \mu\text{m}$. We emphasize that no such change was observed at this wavelength in the preceding experiments. In this technique, a single picosecond pulse at $0.53 \mu\text{m}$ was divided into two parts by a beamsplitter. These two pulses were then recombined so that they were temporally and spatially coincident in the LiIO_3 at an angle $\theta = 1.2^\circ$. The interference of these two pump pulses spatially modulates the electric field which may cause a periodic change in the complex index of refraction of the sample. If such an irradiance dependence is present, each pump beam will be self-diffracted by this laser-induced grating into two first orders at $\pm\theta$. One first order for each pump beam will be scattered into the direction of the other pump, and one will be diffracted in a background-free direction (which we label $-\theta$). There is no signal at $-\theta$ unless a grating is produced by the pump pulses.

The self-diffraction efficiencies as a function of irradiance are shown in figure 4 by the crosses. The crystal was oriented so the $0.53 \mu\text{m}$ beams were incident near the phase-matched condition for down conversion. The irradiances recorded in figure 4 are for one of two equally intense pump beam. Following these measurements, we subsequently blocked one pump beam while continuing to measure the diffraction efficiency of the other pump. The results are the solid dots in figure 4. Clearly, a permanent component to the grating has been produced that continues to diffract light when the modulation of the intensity has been removed. As expected, the diffraction efficiency of the permanent grating is independent of pump irradiance. This grating was not erased by irradiating with a single beam as occurs with photorefractive materials such as BaTiO_3 [5].

In figure 5, we present measurements similar to those of figure 4 except that the crystal has been rotated 78° about the bisector of the angle between the two pump beams, away from the phase-matched orientation. Here the energy in one of the pump beams has been reduced by a factor of six with respect to the other pump. The irradiance quoted in figure 5 is for the strong pump beam. Notice that the measured self-diffraction efficiencies are larger for this orientation and that no permanent grating was observed, even with equally intense pump beams. This dependence of the self-diffracted signal on sample orientation is emphasized in figure 6. Here, the diffraction efficiency is shown as a function of the angle the sample is rotated away from phase-match, as described above.

For this sample thickness ($\sim 5 \text{ mm}$) and this grating spacing ($\sim 25 \mu\text{m}$), we are in the Bragg grating regime. That is, the gratings produced here cannot be considered thin, and the measured self-diffracted signal at $-\theta$ violates the Bragg condition. This makes quantitative analysis of the results of figure 4 - figure 6 difficult. Although not all features of this data are understood by the authors at this time, it is clear that we have observed permanent and transient index (or absorption) changes in the sample at $0.53 \mu\text{m}$. We emphasize once again that these changes are too small to destroy phase match and account for the saturation and turn down in the diffraction efficiency as shown in figure 2.

6. Phase-Matched Second Harmonic Spatial Profiles

Having shown that laser-induced absorptive and index changes (both at 0.53 μm and 1.06 μm) are small, we suspect that the eventual decrease in the diffraction efficiency with increasing 1.06 μm irradiance is caused by down conversion. In this section, we show that this is indeed so.

In these experiments, we monitored the spatial profile of the second harmonic produced by phase matching the LiIO_3 crystal as a function of incident fundamental irradiance. At low incident 1.06 μm irradiance, the profile at 0.53 μm is a smooth Gaussian as shown in figure 7. As the 1.06 μm irradiance is increased past the efficiency maximum (as shown in figure 2), the profile is distorted as shown in figure 8. That is, the second harmonic is skewed to one side. This can be understood by recalling that LiIO_3 possesses a large walk-off angle (4°) between the fundamental and second harmonic when phase matched. For a fundamental beam radius of 0.44 mm (half width at the e^{-2} point in irradiance) and a crystal length of 5 mm, the two beams (fundamental and second harmonic) will be separated by 0.33 mm at the exit surface. This separation is of the order of the 1.06 μm beam radius. Down-conversion would be expected to be important only in regions where the fundamental and second harmonic beams overlap and where both irradiances are large, i.e., near the rear of the crystal. This would produce a lopsided spatial distribution of second harmonic light, as shown in figure 8. We would expect then that by rotating the crystal 180° about the incident beam direction that both the walk-off direction and the distortion would be inverted. That this is the case can be seen in figure 9. From these results, we conclude that parametric down conversion is primarily responsible for limiting the harmonic conversion efficiency [9,10].

7. Conclusions

Laser-induced damage thresholds in LiIO_3 have been determined for two pulsewidths (45 and 145 psec), for two wavelengths (0.53 and 1.06 μm), and for phase-matched and non-phase-matched crystal orientations. Multiple shot thresholds were lower than single-shot thresholds for all pulsewidths, crystal orientations and wavelengths studied. In addition, the multiple shot LID thresholds were lower at 0.53 μm than at 1.06 μm , indicating that the laser-induced threshold is lowered by cumulative defects produced by absorption of the 0.53 μm radiation. Self-diffraction experiments confirmed the presence of both reversible and irreversible changes in the material refractive index prior to damage, even though no nonlinear absorption was resolvable at 0.53 μm for the maximum irradiances available from our system. Higher order nonlinear absorption was, however, observed for 1.06 μm light. We emphasize that this absorption was only observed for 1.06 μm irradiances well above those available at 0.53 μm . Finally, for picosecond optical pulses, the second harmonic conversion efficiency was shown to be limited by optical parametric down conversion - not by nonlinear absorption, index changes that destroy phase matching, or by laser-induced damage.

The authors gratefully acknowledge the support of the Office of Naval Research, The Robert A. Welch Foundation, and the North Texas State Faculty Research Fund. We also thank T. Nowicki and Interactive Radiation Inc. for supplying the LiIO_3 crystals used in these experiments.

8. References

- [1] F. R. Nash, J. G. Bergman, G. D. Boyd, and E. H. Turner, *J. of Appl. Physics*, 40, 5201, 1969.
- [2] E. W. Van Stryland, M. A. Woodall, W. E. Williams, and M. J. Soileau, Proceedings of the 1981 Symposium on Laser Induced Damage, Boulder, Colorado, Nov. 1981.
- [3] J. O. Porteus, J. L. Jerniga, and W. N. Faith, *NBS Spec. Pub.* 509, 507 (1977).
- [4] S.-T. Wu, M. Bass, and J. P. Stone, Proceedings of the 1981 Symposium on Laser Induced Damage; Boulder, Colorado, November 1981.
- [5] Jack Feinberg, D. Heuman, A. R. Tanguay, and R. W. Hellwarth, *J. Appl. Phys.* 51, 1297 (1980).
- [6] G. Nath, H. Mehmanesch, and M. Bsaager, *Appl. Phys. Lett.* 17, 286 (1970).
- [7] Christine A. Schwartz, Jean-Louis Oduar, and Edmond M. Batifol, *IEEE J. Quantum Elec.* QE-11, 616, 1975.
- [8] V. G. Dimitriev and V. A. Konovolov, *Sov. J. Quantum Elec.* 9, 300, 1979.
- [9] J. A. Armstrong, N. Bloembergen, J. Ducuing, and P. S. Pershan, *Phys. Rev.* 127, 1918 (1962).
- [10] R. Stephen Craxton, *IEEE, J. Quantum Elec.*, QE-17, 1771, 1981.
- [11] N. M. Bitzurius, V. I. Bredikhin, and V. N. Genkin, *Sov. J. Quantum. Elec.* 8, 1377, 1978.

Figure Captions

- Figure 1. Second harmonic conversion efficiency χ 's as a function of irradiance, and $1.06 \mu\text{m}$ transmission \bullet 's as a function of irradiance.
- Figure 2. Inverse cube of the transmission versus the cube of the incident $1.06 \mu\text{m}$ irradiance.
- Figure 3. Diffraction efficiency in a light by light scattering experiment versus the irradiance of the of the pump beam as explained in section 5. Crosses indicate data taken with irradiance increasing. Dots indicate one beam blocked and irradiance decreasing.
- Figure 4. Diffraction efficiency in a light by light scattering experiment versus incident irradiance of the strong pump beam with the crystal rotated 90° about the beam axis from the arrangement used to obtain the data of figure 4.
- Figure 5. Diffraction efficiency versus the angle about the beam direction as described in section 5. Both pump beams were equally intense for this measurement.
- Figure 6. Two-dimensional spatial beam profile of the second harmonic produced in LiIO_3 at low irradiance.
- Figure 7. Two-dimensional spatial beam profile of the second harmonic produced in LiIO_3 at high irradiance.
- Figure 8. Two-dimensional spatial beam profile of the second harmonic produced in LiIO_3 at high irradiance. The crystal has been rotated 180° about the beam axis from the position used in figure 8 as described in section 6.

TABLE I

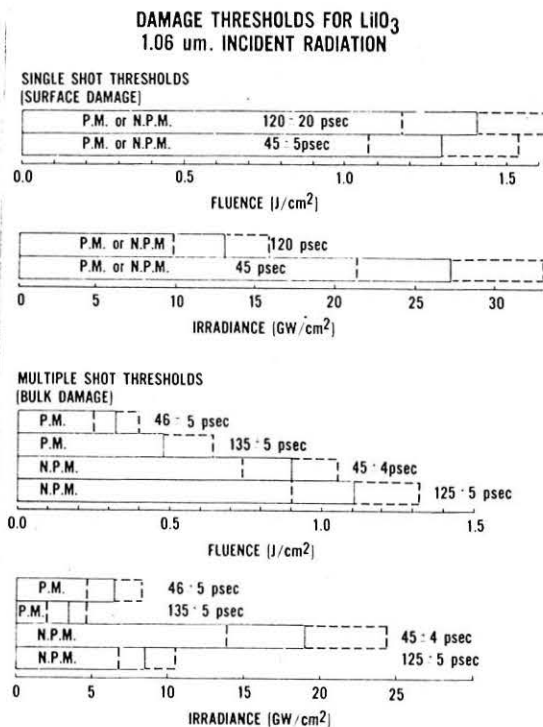
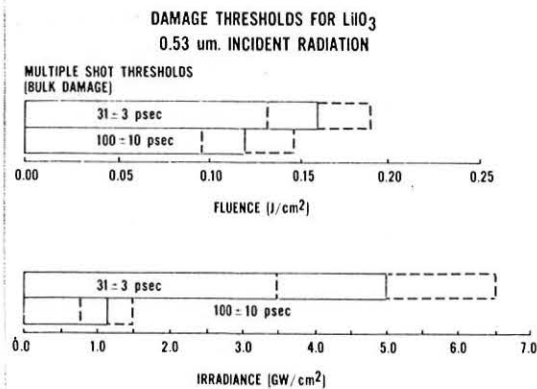


TABLE II



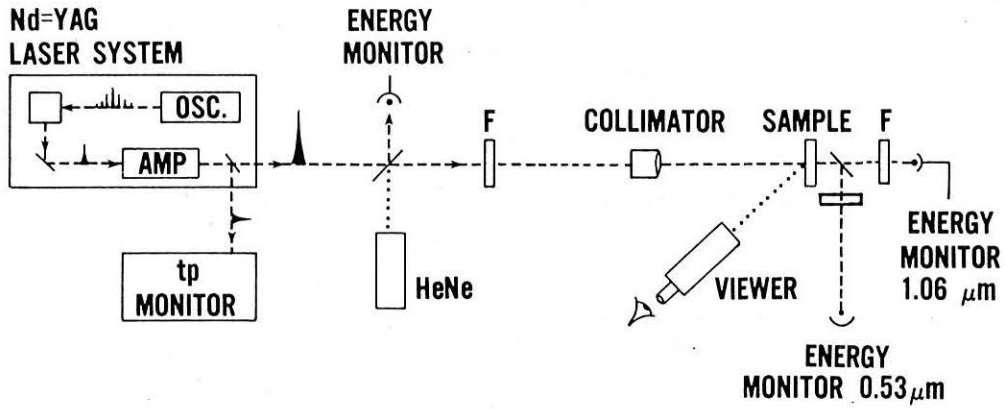


Figure 1

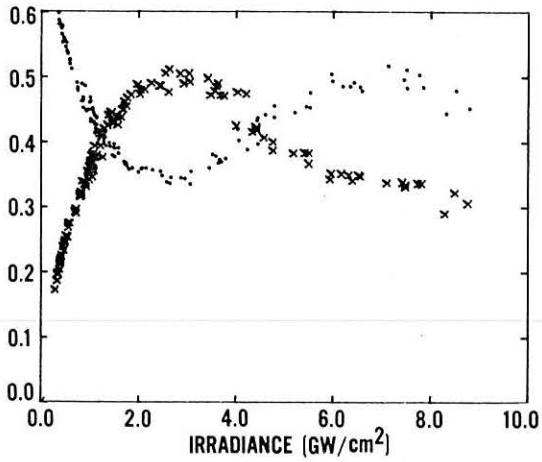


Figure 2

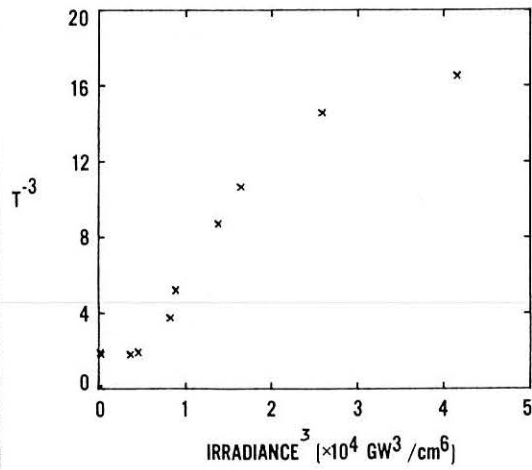


Figure 3

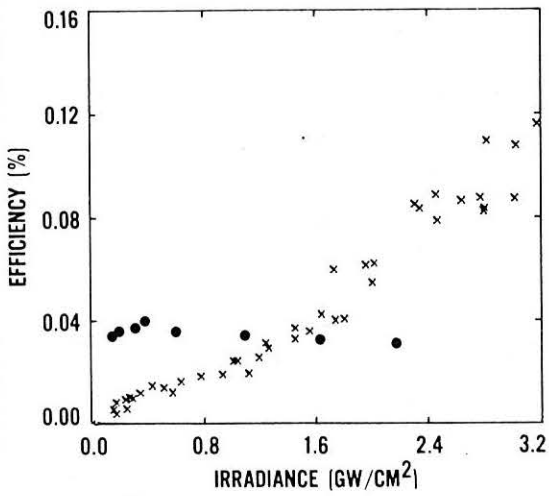


Figure 4

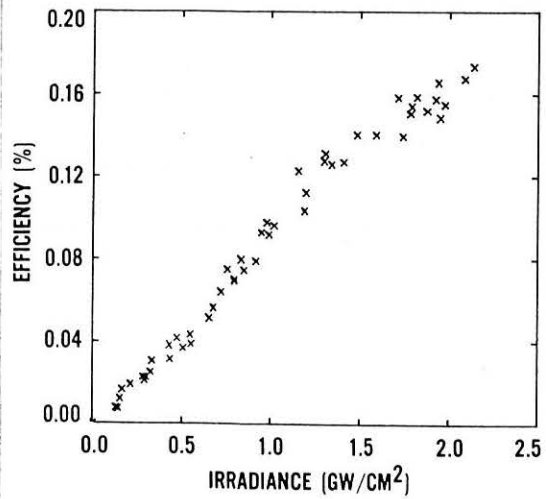


Figure 5

COMPARISON OF THE SHEET

THE SHEET TYPE AND THE TYPE OF THE SHEET

THE SHEET TYPE AND THE TYPE OF THE SHEET

THE SHEET TYPE AND THE TYPE OF THE SHEET

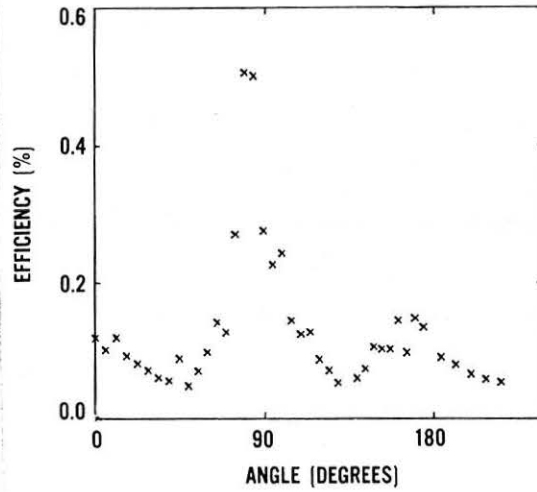


Figure 6

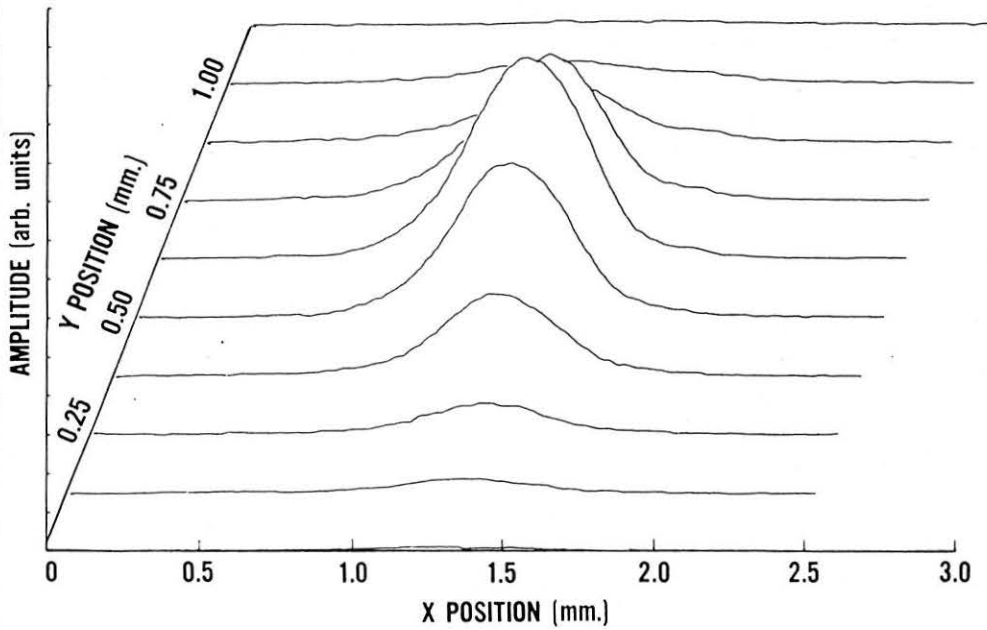


Figure 7

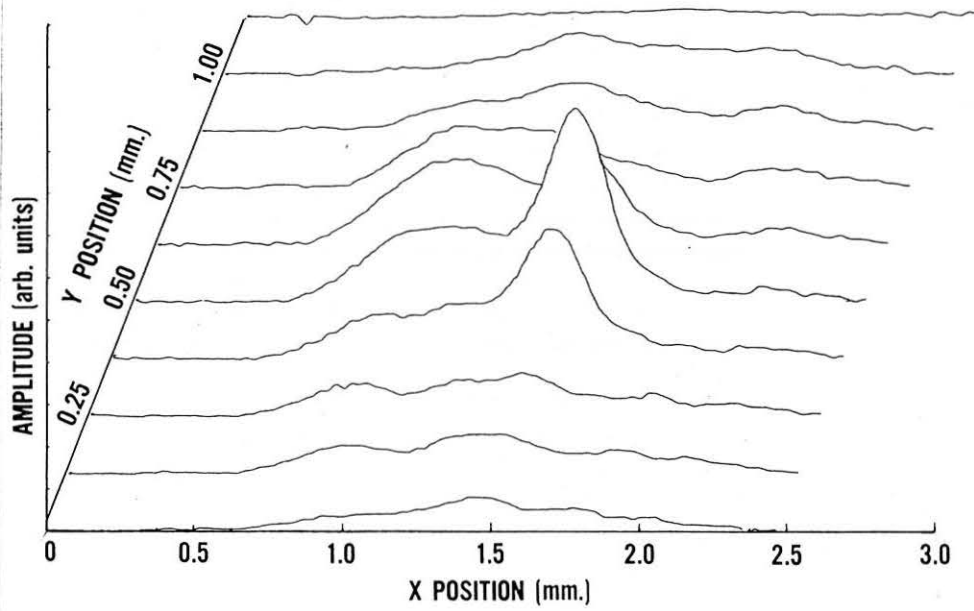


Figure 8

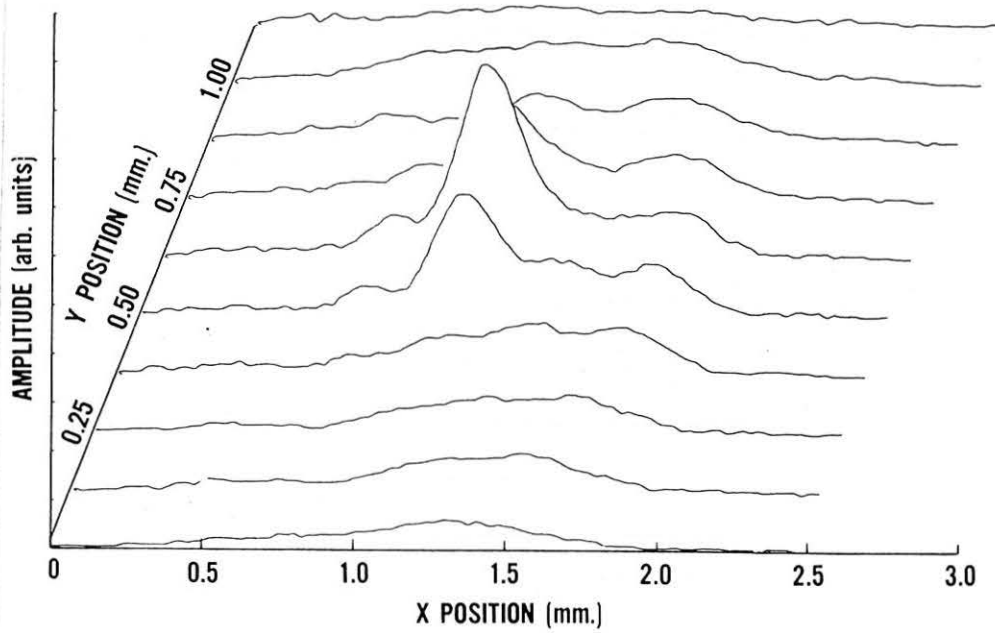


Figure 9